Inductive Measurement of Optically Hyperpolarized Phosphorous Donor Nuclei in an Isotopically Enriched Silicon-28 Crystal

P. Gumann,[1,2,3,*] O. Patange,[1,2,4] C. Ramanathan,[5,†] H. Haas,[1,2] O. Moussa,[1,2] M. L. W. Thewalt,[6] H. Riemann,[7] N. V. Abrosimov,[7] P. Becker,[8] H.-J. Pohl,[9] K. M. Itoh,[10] and D. G. Cory[1,2,4,11,12,13]

[1]*Institute for Quantum Computing, University of Waterloo, Waterloo, Ontario N2L 3G1, Canada*
[2]*Department of Physics and Astronomy, University of Waterloo, Waterloo, Ontario N2L 3G1, Canada*
[3]*Department of Physics, Harvard University, Cambridge, Massachusetts 02138, USA*
[4]*Waterloo Institute for Nanotechnology, University of Waterloo, Waterloo, Ontario N2L 3G1, Canada*
[5]*Department of Physics and Astronomy, Wilder Laboratory, Dartmouth College, Hanover, New Hampshire 03755, USA*
[6]*Department of Physics, Simon Fraser University, Burnaby, British Columbia V5A 1S6, Canada*
[7]*Leibniz-Institut fuer Kristallzuechtung, 12489 Berlin, Germany*
[8]*PTB Braunschweig, 38116 Braunschweig, Germany*
[9]*VITCON Projectconsult GmbH, 07743 Jena, Germany*
[10]*School of Fundamental Science and Technology, Keio University, Yokohama, 3-14-1 Hiyoshi 223-8522, Japan*
[11]*Canadian Institute for Advanced Research, Toronto, Ontario M5G 1Z8, Canada*
[12]*Department of Chemistry, University of Waterloo, Waterloo, Ontario N2L 3G1, Canada*
[13]*Perimeter Institute for Theoretical Physics, Waterloo, Ontario N2L 2Y5, Canada*

(Received 27 July 2014; revised manuscript received 22 September 2014; published 30 December 2014)

We experimentally demonstrate the first inductive readout of optically hyperpolarized phosphorus-31 donor nuclear spins in an isotopically enriched silicon-28 crystal. The concentration of phosphorus donors in the crystal was 1.5×10^{15} cm^{-3}, 3 orders of magnitude lower than has previously been detected via direct inductive detection. The signal-to-noise ratio measured in a single free induction decay from a 1 cm^3 sample ($\approx 10^{15}$ spins) was 113. By transferring the sample to an X-band ESR spectrometer, we were able to obtain a lower bound for the nuclear spin polarization at 1.7 K of ~64%. The ^{31}P-T_2 measured with a Hahn echo sequence was 420 ms at 1.7 K, which was extended to 1.2 s with a Carr Purcell cycle. The T_1 of the ^{31}P nuclear spins at 1.7 K is extremely long and could not be determined, as no decay was observed even on a time scale of 4.5 h. Optical excitation was performed with a 1047 nm laser, which provided above-band-gap excitation of the silicon. The buildup of the hyperpolarization at 4.2 K followed a single exponential with a characteristic time of 577 s, while the buildup at 1.7 K showed biexponential behavior with characteristic time constants of 578 and 5670 s.

DOI: 10.1103/PhysRevLett.113.267604 PACS numbers: 76.30.Lh, 76.60.Lz

Nuclear spin defects are archetypal models of qubits in solid state systems. We expect them to have long coherence times and to be well controlled [1,2]. However, to date they have mainly been studied via their interaction to a neighboring electron spin [1–4]. Such experiments are indirect probes of the local fields seen by the nuclear spins. Here, we directly observe nuclear spin defects in a dilute sample of silicon, and through a combination of free induction decay (FID) and echo measurements we characterize the local field and its fluctuations.

The phosphorus donor impurity in silicon is a potentially promising candidate for a hybrid quantum information processor [5]. In natural abundance bulk silicon, the 300–600 μs coherence time of the donor electron spin at low temperatures has been shown to be limited primarily by spectral diffusion due to the ^{29}Si nuclei (4.7% natural abundance) [6]. Similar coherence times have also been measured at the level of individual donors [3,4]. In the bulk, this coherence time has been extended to 0.6 s by isotopically engineering the silicon lattice to reduce the ^{29}Si nuclear spin concentration and simultaneously reduce the donor concentration to minimize the dipolar coupling between electron spin donors (thus reducing instantaneous diffusion effects) [7]. The ^{31}P donor nuclear spin has also been shown to have extremely long coherence times (180 s at low temperature and $B = 845$ G) [8], limited primarily by electron spin fluctuations. By ionizing the donors with below-gap narrow-line laser excitation and using dynamical decoupling techniques, the phosphorus nuclear spin coherence times were extended to 39 min at room temperature and 3 h at 4.2 K in a silicon-28 lattice, at ~845 G [9].

It has recently been shown that it is possible to optically hyperpolarize the ^{31}P donor nuclear spins in silicon at relatively low doping concentrations ($\sim 10^{15}$ cm^{-3}) in two different regimes. At high magnetic field (~8.5 T), the phosphorus nuclear spins were detected by using both electron spin resonance (ESR) and electrically detected magnetic resonance (EDMR) [10–13] under white light illumination. The optical nuclear hyperpolarization of −68% built up over a characteristic time of 120 s [12].

Because of the limited penetration of the light into the silicon, the hyperpolarization occurred primarily near the illuminated surface. At low magnetic fields, the nuclear spin polarization (86%) was measured by using photoluminescence excitation spectroscopy with both resonant and above-band-gap laser excitation [8,14,15] and showed subsecond optical hyperpolarization time scales.

Here we demonstrate the direct inductive readout of the phosphorus nuclear magnetic resonance (NMR) signal at a phosphorus donor concentration of $\sim 10^{15}$ cm^{-3} [16], following hyperpolarization of bulk ^{31}P nuclei using nonresonant infrared laser excitation, at high field and low temperature. Previous direct NMR measurements of phosphorus nuclear spins in silicon have been possible only at very high doping concentrations ($\sim 10^{18}$ cm^{-3}) [17,18], about 3 orders of magnitude higher than the concentrations used in this Letter. This inductive readout of the phosphorus donor nuclei allows us to measure nuclear spin properties in the bulk of the sample.

We used a simple NMR detection setup where a cylindrical ^{28}Si-enriched crystal [19] with a phosphorus concentration of 1.5×10^{15} cm^{-3} (boron concentration $\sim 1.0 \times 10^{14}$ cm^{-3}, dislocation-free crystal) was placed in a rhodium-flashed, silver-plated copper, rf coil, wired to a low temperature LC circuit. All experiments presented here were performed at temperatures 4.2 or 1.7 K $\pm$ 0.3 K, and the magnetic field was 6.71 T. The buildup of the high ^{31}P-spin polarization was accomplished by illuminating the sample with a 100 mW, 1047 nm, above-band-gap laser, with a linearly polarized beam of 8 mm effective size (see Supplemental Material [20]). The (indirect) band gap in silicon is 1.12 eV which corresponds to an optical wavelength of 1100 nm. The penetration depth for 1047 nm light in silicon at cryogenic temperatures is a few centimeters which allowed the excitation of bulk phosphorus impurities [27].

The effective Hamiltonian of the phosphorus donor impurity at high magnetic field is

$$\mathcal{H} = -\gamma_n B_z I_z - \gamma_e B_z S_z + \frac{2\pi}{\hbar} A S_z I_z, \qquad (1)$$

where $\gamma_n/2\pi = 17.23$ MHz/T and $\gamma_e/2\pi = -28.024$ GHz/T are the nuclear and electron gyromagnetic ratios, respectively, and $A = 117.54$ MHz is the isotropic hyperfine interaction term. In the high-field limit, the eigenstates are almost exactly given by the product states $|\uparrow_e\uparrow_n\rangle$, $|\uparrow_e\downarrow_n\rangle$, $|\downarrow_e\uparrow_n\rangle$, and $|\downarrow_e\downarrow_n\rangle$ [28]; see Fig. 1(b). At 6.71 T, the thermal electron spin polarization is 79% at 4.2 K and 99% at 1.7 K, while the thermal nuclear spin polarization is 0.07% at 4.2 K and 0.16% at 1.7 K. We probed the nuclear spins in the lower spin electron manifold, transition $\nu_{n_1} = 174.08$ MHz [see Fig. 1(b)].

Figure 1(c) illustrates the experimental sequence used to measure the buildup of the phosphorus hyperpolarization. Following a saturation train of $\pi/2$ pulses to destroy the remnants of the hyperpolarization from the previous

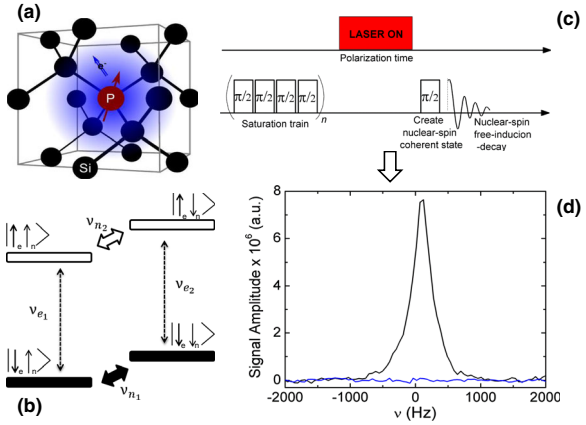

FIG. 1 (color online). Raw spectrum of ^{31}P-nuclear spins in ^{28}Si crystal, at 1.7 K in 6.7 T. The data were taken by applying only one $\pi/2$ pulse and recording the FID. The signal-to-noise ratio is 113. (a) Schematic and (b) electronic structure of the donor impurity. (c) Pulse sequence used to obtain the spectrum in (d) (the blue line/base line is the data with the laser off).

experiment, the nuclear spins are polarized with laser irradiation. The NMR signal was measured by using a single $\pi/2$ rf pulse (duration 8.5 μs), and the resulting free induction decay was Fourier transformed to produce the NMR spectrum. A typical signal is show in Fig. 1(d), produced with 200 s laser irradiation. The full line width at half maximum (FWHM) is $\sim$160 Hz (consistent with $T_2^* \sim 2$ ms).

The buildup of the hyperpolarization was measured by varying the laser excitation time (or polarization time), from 2 s to 10 h (Fig. 2). This buildup was measured at both 4.2 and 1.7 K. The ratio of the steady state signals at these temperatures was measured to be 5.88. We were able to fit the buildup curve at 4.2 K by using a single exponential fit with a characteristic time of 577 s. The measured buildup at 1.7 K showed biexponential behavior, with characteristic times of 578 and 5670 s. The relative contributions of the two components were 57.3% and 42.7%, respectively. Comparing the amplitude of the short time constant component at 1.7 K with the signal at 4.2 K, both of which had similar growth times, indicates an enhancement of 3.78. Assuming a simple Boltzmann scaling of the electron spin polarization, lowering the temperature from 4.2 to 1.7 K should just change the polarization by a factor of 1.25.

There are at least two contributions to this additional enhancement. First, the efficiency of coupling the laser to the silicon crystal is improved at low temperature, as the liquid helium bath enters a superfluid phase below 2.17 K and consequently bubbles in the bath are eliminated. At 4.2 K, we in fact observe substantial bubbling of the liquid helium at the inner window of the Dewar. These bubbles reduce the effective coupling of the light onto the sample. In addition, the electron spin T_1 is longer at low temperature [7], and the interplay with the optically excited carriers could enhance the polarization [29,30].

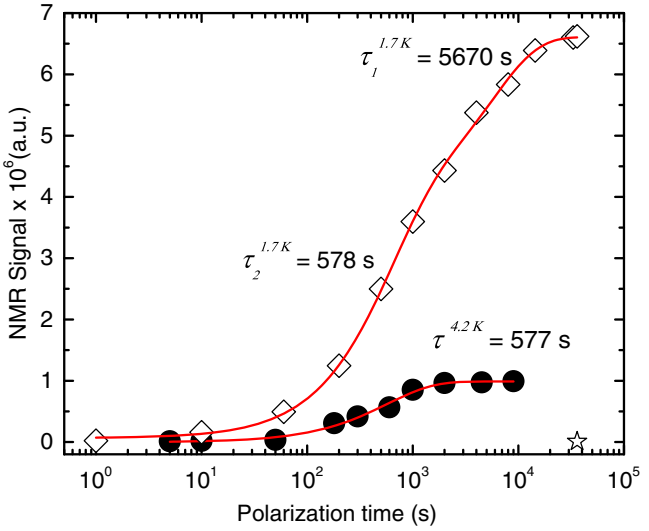

FIG. 2 (color online). Buildup on the nuclear spin polarization by 1047 nm laser irradiation for up to ~10 h, at 1.7 and 4.2 K temperature, respectively. The red lines represent a biexponential fit with time constants, $\tau_1 = 5670$ s and $\tau_2 = 578$ s at 1.7 K, and an exponential fit with $\tau = 577$ s at 4.2 K. The star represents a thermal polarization measurement (laser off) for ~10 h, at 1.7 K, where no polarization could be observed.

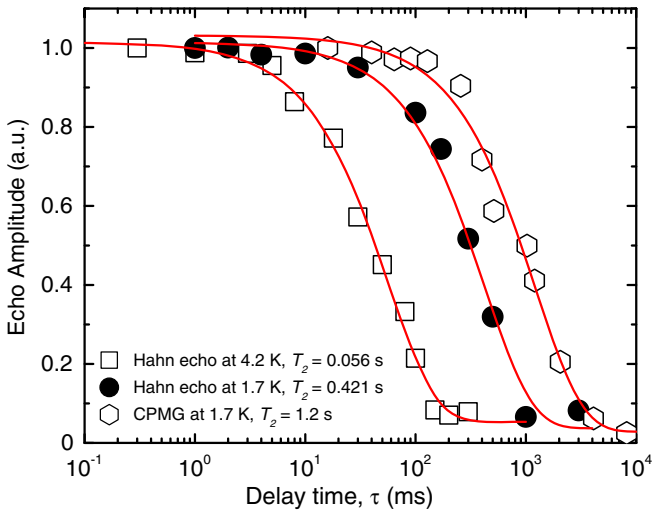

FIG. 3 (color online). Nuclear spin coherence time T_2 measured with the Hahn echo at 4.2 K temperature (open squares); Hahn echo at 1.7 K (full circles); and CPMG pulse sequence at 1.7 K (open hexagons). All data were measured in 6.7 T field, with 200 s of optical polarization provided by a 1047 nm, 100 mW, above-gap laser.

The detailed physics underlying the optical hyperpolarization process is not well understood. Honig and co-workers have previously shown that the negatively ionized donors produced by spin trapping of optically excited conduction band electrons form singlet states at high field [29]. Similarly, optical experiments have shown the creation of donor-bound excitons at both low [14] and high magnetic fields [31], and the electron pairs in these donor-bound excitons also form singlets. When the electron spin polarization (of the donors and free electrons) is high, it is necessary to flip either the donor or the free electron to form the bound singlet. Sekiguchi *et al.* have suggested that when spin-orbit interactions are weak, as in silicon, this trapping process is most likely mediated by the hyperfine interaction, resulting in the hyperpolarization of the nuclear spins [31]. Alternatively, the hyperpolarization could be produced by cross relaxation of the donors, as they are heated up by the optically excited conduction band electrons [32,33].

The long time component of the growth curve observed at 1.7 K was not measured beyond 2.5 h polarization time at 4.2 K (Fig. 2). A similar biexponential growth has been observed in a recent microwave-induced dynamic nuclear polarization (DNP) experiment on phosphorus donors in natural abundance silicon (doping concentration of 6.5×10^{16} cm^{-3}) at 4.6 T and temperatures of 200 mK and 1 K [34]. They observed a short time scale of 15 s and a longer time scale of 1100 s in their experiment. Though they attribute the presence of the longer time scale to the presence of ^{29}Si spins around the phosphorus donors, this is unlikely to be the case here, as a similar biexponential behavior is observed in our isotopically enriched silicon-28 crystal.

We were unable to measure the signal from the phosphorus nuclei in the absence of hyperpolarization, making it difficult to directly quantify either the sign or the magnitude of the nuclear spin polarization. In order to estimate the phosphorus nuclear spin polarization, we moved the sample to an *X*-band cw-ESR spectrometer following optical excitation at 4.2 K for 3 h at 6.71 T. The resulting ESR spectrum, measured at 4.2 K, is shown in Fig. 2 of Supplemental Material [20]. The magnitude of the measured phosphorus polarization, calculated from the difference in the integrated intensities of the two ESR lines, is −11%, which is the lower bound for the induced hyperpolarization at 4.2 K, as some of the polarization will have decayed as the sample was removed from the 6.71 T field and warmed up, before being cooled back down in the ESR cryostat. This indicates a lower bound of ~64% (11×5.88) for the polarization at 1.7 K. The negative sign of the hyperpolarization, indicated by the higher intensity of the high-field line compared to the low-field line, is in agreement with prior high-field EDMR results [11,35].

We performed spin-echo experiments to measure the coherence time of the ^{31}P nuclear spins. Following 200 s of laser irradiation, a Hahn-echo sequence ($\pi/2 - \tau - \pi - \tau -$ acquire) was used to measure the nuclear spin coherence time (Fig. 3). By recording the echo signal while varying the delay time (τ), we measured the signal decay at both 4.2 and 1.7 K as shown in Fig. 3. We fit the data with a single exponential decay and measured nuclear spin T_2 values of 56 and 421 ms at 4.2 and 1.7 K, respectively.

As the magnetic field is increased, it is observed that the electron spin T_1 at low temperature and high field gets

significantly shorter, since $T_1^{-1} \propto B^4$ as the result of a direct single-phonon relaxation process [36–39]. The hyperfine interaction is field independent, so the main factor limiting the nuclear T_2 is the electron T_1 carrying the ^{31}P spin to the electron spin $|\uparrow_e\rangle$ manifold [40] (see Supplemental Material [20] for details). In the presence of light, the T_1 is further shortened by up to 2 orders of magnitude due to trapping and reemission, with T_1 on the order of 2 ms in the presence of light and almost 20 ms in the dark at 8.56 T [11,35].

Here the electron spin undergoing T_1 relaxation induces an effective T_2 process on the nuclear spin with time constant T_2^{en} (see Supplemental Material [20]). If $AT_1^e \gg 1$, then

$$T_2^{en} = \frac{T_1^e}{p_\uparrow},$$

where $p_\uparrow$ is the probability for the electron to be in the excited state. The high temperature limit of this model has been applied to explain the nuclear T_2 [1]. If we assume that the experimentally observed nuclear $T_2(T)$ combines two independent effects $1/T_2(T) = 1/T_2' + p_\uparrow(T)/T_1^e(T)$, where T_2' is temperature independent, then we obtain $1/T_2' \leq 1/T_2(1.7\ \mathrm{K})$. This in turn puts an upper bound on the electron relaxation time $T_1^e(4.2\ \mathrm{K}) \leq p_\uparrow(4.2\ \mathrm{K})((T_2(1.7\ \mathrm{K})T_2(4.2\ \mathrm{K}))/(T_2(1.7\ \mathrm{K}) - T_2(4.2\ \mathrm{K})))$ or $T_1^e(4.2\ \mathrm{K}) \leq 6.7$ ms, where we have assumed that $p_\uparrow$ is given by the equilibrium thermal probability. This value is shorter than the $T_1^e = 20$ ms measured in the dark at 8.56 T [35].

In order to minimize the effect of environmental fluctuations, we applied a Carr-Purcell-Meiboom-Gill (CPMG) refocusing pulse sequence to extend the nuclear spin coherence time. In the CPMG sequence, the single π pulse of the Hahn echo is substituted with a series of π pulses that are 90° out of phase with respect to each other, with a τ spacing of 2 ms. The resulting echo decay is presented in Fig. 3, with a single exponential fit to the data returning $T_2 = 1.2\ \mathrm{s} \pm 0.1$ s, a factor of almost 3 improvement in nuclear spin coherence time. This is similar to the value of 1.75 s measured previously by using endor at 5.5 K [1]. This CPMG sequence will refocus interactions between the phosphorus nucleus and other spins (or fields) that are fluctuating on a time scale longer than a few hundred hertz. The sequence will thus refocus fluctuations due to distant donor electrons, silicon nuclei (the silicon-phosphorus nuclear dipolar coupling is very small and does not play an important role here [41]), and static field inhomogeneities. The phosphorus nuclear dipolar coupling is not refocused but is only about 1.5 mHz for our donor concentration, and the dominant contribution from the electron T_1^e induced nuclear T_2 is also not refocused by the CPMG sequence.

Last, we confirmed the long T_1 relaxation times, at 4.2 and 1.7 K temperatures. Figure 4 shows T_1 data for two experiments, a 200 s laser polarization pulse, followed by in the first case a delay time τ and a $\pi/2$-readout pulse and in the second case π-τ-$\pi/2$ pulse sequence. The only difference between the two runs is the initial nuclear state. If most of the population is localized in the $|\downarrow_e\uparrow_n\rangle$ state, applying a π pulse before the readout pulse will move it to the $|\downarrow_e\downarrow_n\rangle$ state [Fig. 1(b)]. The T_1 relaxation should not depend on the initial state, which is confirmed in Fig. 4. In addition, we observe that the spin-lattice relaxation time not only increases at lower temperatures but also exceeds the measuring times of our setup; no visible decay was observed after waiting for delay time $\tau = 4.5$ h (Fig. 4).

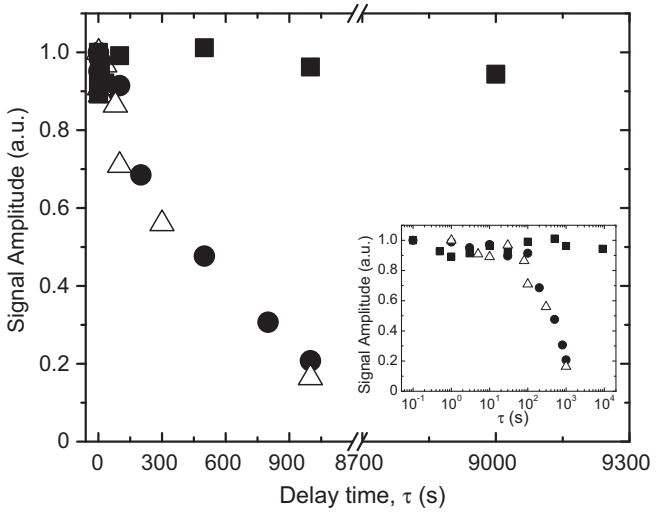

FIG. 4. Nuclear spin relaxation time T_1 measured with a simple $\pi/2$ readout pulse at 4.2 (open triangles) and 1.7 K (black squares), respectively, and with an inversion recovery pulse sequence (closed circles) at 4.2 K.

In conclusion, the results presented here show the first single FID measurement of the local magnetic fields seen by ^{31}P nuclear spins in a dilute crystal of ^{28}Si. The negative ^{31}P polarization is $> 11\%$ at 4.2 K, and $> 64\%$ at 1.7 K and 6.71 T. It was accomplished by directly illuminating the sample with an above-gap 1047 nm laser for over 5 h at 1.7 K and 2.7 h at 4.2 K. We were able to extend the T_2 relaxation time to 1.2 s at 1.7 K and confirm an extremely long T_1 of the ^{31}P nuclear spins at 1.7 K which could not be determined within the time scale of this experiment.

This work was supported by the Natural Sciences and Engineering Research Council of Canada (NSERC), Canadian Excellence Research Chairs (CERC) Program and the Canadian Institute for Advanced Research (CIFAR) and Industry Canada. C.R. acknowledges support of a Junior Faculty Fellowship from Dartmouth College. The ^{28}Si-enriched sample used in this study was prepared from Avo28 material produced by the International Avogadro Coordination (IAC) Project (2004–2011) in cooperation among the BIPM, the IN-RIM (Italy), the IRMM (EU), the NMIA (Australia), the NMIJ (Japan), the NPL (UK), and the PTB (Germany).

*gumann@physics.harvard.edu
†chandrasekhar.ramanathan@dartmouth.edu

[1] J. J. L. Morton, A. M. Tyryshkin, R. M. Brown, S. Shankar, B. W. Lovett, A. Ardavan, T. Schenkel, E. E. Haller, J. W. Ager, and S. A. Lyon, Nature (London) **455**, 1085 (2008).
[2] D. D. Awschalom, L. C. Bassett, A. S. Dzurak, E. L. Hu, and J. R. Petta, Science **339**, 1174 (2013).
[3] J. T. Muhonen *et al.*, Nat. Nanotechnol. **9**, 986 (2014).
[4] J. J. Pla, K. Y. Tan, J. P. Dehollain, W. H. Lim, J. J. L. Morton, F. A. Zwanenburg, D. N. Jamieson, A. S. Dzurak, and A. Morello, Nature (London) **496**, 334 (2013).
[5] B. E. Kane, Nature (London) **393**, 133 (1998).
[6] A. M. Tyryshkin, J. J. L. Morton, S. C. Benjamin, A. Ardavan, G. A. D. Briggs, J. W.Ager, and S. A. Lyon, J. Phys. Condens. Matter **18**, S783 (2006).
[7] A. M. Tyryshkin *et al.*, Nat. Mater. **11**, 143 (2012).
[8] M. Steger, K. Saeedi, M. L. W. Thewalt, J. J. L. Morton, H. Riemann, N. V. Abrosimov, P. Becker, and H.-J. Pohl, Science **336**, 1280 (2012).
[9] K. Saeedi, S. Simmons, J. Z. Salvail, P. Dluhy, H. Riemann, N. V. Abrosimov, P. Becker, H.-J. Pohl, J. J. L. Morton, and M. L. W. Thewalt, Science, **342**, 830 (2013).
[10] C. C. Lo, C. D. Weis, J. van Tol, J. Bokor, and T. Schenkel, Phys. Rev. Lett. **110**, 057601 (2013).
[11] G. W. Morley, D. McCamey, H. Seipel, L.-C. Brunel, J. van. Tol, and C. Boehme, Phys. Rev. Lett. **101**, 207602 (2008).
[12] D. R. McCamey, J. van Tol, G. W. Morley, and C. Boehme, Phys. Rev. Lett. **102**, 027601 (2009).
[13] D. R. McCamey, J. V. Tol, G. W. Morley, and C. Boehme, Science **330**, 1652 (2010).
[14] A. Yang, M. Steger, T. Sekiguchi, M. Thewalt, T. Ladd, K. Itoh, H. Riemann, N. Abrosimov, P. Becker, and H.-J. Pohl, Phys. Rev. Lett. **102**, 257401 (2009).
[15] A. Yang *et al.*, Phys. Rev. Lett. **97**, 227401 (2006).
[16] L. Dreher, F. Hoehne, M. Stutzmann, and M. S. Brandt, Phys. Rev. Lett. **108**, 027602 (2012).
[17] H. Alloul and P. Dellouve, Phys. Rev. Lett. **59**, 578 (1987).
[18] M. Jeong, M. Song, T. Ueno, T. Mizusaki, A. Matsubara, and S. Lee, J. Phys. Conf. Ser. **150**, 042078 (2009).
[19] P. Becker, H.-J. Pohl, H. Riemann, and N. Abrosimov, Phys. Status Solidi (a) **207**, 49 (2010).
[20] See Supplemental Material at for http://link.aps.org/supplemental/10.1103/PhysRevLett.113.267604, which includes Refs. [21–26], for theoretical description of the nuclear spin T_2 due to the electron spin undergoing T_1 relaxation model, the data on the nuclear T_2 relaxation with the laser on, and the technical description of the optical, NMR, and cw-ESR setup including a short sample description.
[21] H.-P. Breuer and F. Petruccione, *The Theory of Open Quantum Systems* (Oxford University, New York, 2002).
[22] G. Lindblad, Commun. Math. Phys. **48**, 119 (1976).
[23] C. A. Brasil, F. F. Fanchini, and R. de Jesus Napolitano, Rev. Bras. Ensino Fis. **35**, 1 (2013).
[24] P. Pearle, arXiv:1204.2016v1 [Eur. J. Phys. (to be published)].
[25] M. A. Nielsen and I. L. Chuang, *Quantum Computation and Quantum Information* (Cambridge University Press, Cambridge, England, 2000).
[26] H.-J. Briegel and B.-G. Englert, Phys. Rev. A **47**, 3311 (1993).
[27] G. G. MacFarlane, T. P. McLean, J. E. Quarrington, and V. Roberts, J. Phys. Chem. Solids **8**, 388 (1959).
[28] A. Schweiger and G. Jeschke, *Principles of Pulse Electron Paramagnetic Resonance* (Oxford University Press, New York, 2001).
[29] D. D. Thornton and A. Honig, Phys. Rev. Lett. **30**, 909 (1973).
[30] A. Honig and N. Lagnado, in *Proceedings of the Tenth International Conference on the Physics of Semiconductors, Cambridge, Massachusetts, 190*, edited by S. P. Keller, J. C. Hensel, and F. Stern (U.S. AEC Division of Technical Information, Springfield, VA, 1970), p. 809.
[31] T. Sekiguchi, M. Steger, K. Saeedi, M. L. W. Thewalt, H. Riemann, N. V. Abrosimov, and N. Nötzel, Phys. Rev. Lett. **104**, 137402 (2010).
[32] G. Feher, Phys. Rev. Lett. **3**, 135 (1959).
[33] D. Pines, J. Bardeen, and C. Slichter, Phys. Rev. **106**, 489 (1957).
[34] J. Järvinen *et al.*, Phys. Rev. B **90**, 214401 (2014).
[35] D. R. McCamey, C. Boehme, G. W. Morley, and J. van Tol, Phys. Rev. B **85**, 073201 (2012).
[36] A. Honig and E. Stupp, Phys. Rev. Lett. **1**, 275 (1958).
[37] A. Honig and E. Stupp, Phys. Rev. **117**, 69 (1960).
[38] L. M. Roth, Phys. Rev. **118**, 1534 (1960).
[39] H. Hasegawa, Phys. Rev. **118**, 1523 (1960).
[40] We are in the processes of extending the ^{31}P T_2 by moving the polarized system to higher temperature where the T_1 of the electron becomes much less important to the defect T_2.
[41] Given the isotopic enrichment of 99.9954% for the silicon-28, we assume that the residual 0.0046% is purely silicon-29 as the concentration of silicon-30 has been measured to be about 40 times lower than that of silicon-29 in the Avogadro samples [42]. Assuming a uniform distribution of spins, this yields an average nearest neighbor silicon hyperfine coupling of about 200 kHz, average nearest neighbor silicon nuclear dipolar coupling of about 7 Hz, and average nearest neighbor silicon-phosphorus nuclear dipolar coupling of 100 Hz.
[42] R. D. Vocke, S. A. Rabb, and G. C. Turk, Metrologia **51**, 361 (2014).